THE JOURNAL OF BIOLOGICAL CHEMISTRY VOL. 283, NO. 12, pp. 7885–7893, March 21, 2008

Kinetic Analysis of the Interaction of the C1 Domain of Protein Kinase C with Lipid Membranes by Stopped-flow Spectroscopy*[S]

Received for publication, December 5, 2007, and in revised form, January 9, 2008 Published, JBC Papers in Press, January 10, 2008, DOI 10.1074/jbc.M709943200

Daniel R. Dries[‡1] **and Alexandra C. Newton**[§2]

From the [‡]*Biomedical Sciences Graduate Program and the* [§]*Department of Pharmacology, University of California at San Diego, La Jolla, California 92093*

The diacylglycerol (DG)/phorbol ester-dependent translocation of conventional protein kinase C (PKC) isozymes is mediated by the C1 domain, a membrane-targeting module that also selectively binds phosphatidylserine (PS). Using stopped-flow spectroscopy, we dissect the contribution of DG/phorbol esters (C1 ligand) and PS in driving the association and dissociation of the C1 domain from membranes. Specifically, we examine the binding to membranes of the C1B domain of PKCβ with a substituted Trp (Y123W) whose fluorescence is quenched upon binding to membranes. Binding of this construct (C1Bβ-Y123W) to phospholipid vesicles is cooperative with respect to PS content and dependent on C1 ligand, as previously characterized. Stopped-flow analysis reveals that the apparent association rate (k_{on}^{app}), but not the apparent dissociation rate (k_{off}^{app}), is highly sensitive to PS content: the 60-fold increase in membrane affinity for vesicles containing no PS compared with 40 mol % PS results primarily from a robust (30-fold) increase in k_{on}^{app} with little effect (2-fold) on k_{off}^{app}. Membrane affinity is also controlled by the content and structure of the C1 ligand. In contrast to PS, these ligands markedly alter k_{off}^{app} with smaller effects on k_{on}^{app}. We also show that the affinity for phorbol ester-containing membranes is 2 orders of magnitude higher than that for DG-containing membranes primarily resulting from differences in k_{off}^{app}. Our data are consistent with a model in which the C1 domain is recruited to the membrane via an initial weak electrostatic interaction with PS, followed by a rapid two-dimensional search for ligand, the binding of which retains the domain at the membrane. Thus, PS drives the initial encounter, and DG/phorbol esters retain the domain on membranes. The decreased effectiveness of DG compared with phorbol esters in retaining the C1 domain on membranes contributes to the molecular dichotomy of the rapid, transient nature of DG-dependent PKC signaling *versus* the chronic hyperactivity of phorbol ester-activated PKC.

The activity of PKC[3] is critical to many signaling pathways, through which PKC elicits a variety of physiological outputs (1, 2). Whereas PKC may be constitutively activated through proteolysis, the principal mechanism for the activation of the conventional (α, the alternatively spliced βI and βII, γ) and novel (δ, ϵ, θ, η) PKC isozymes is via translocation of PKC to the membrane; this translocation is driven by the C1 domain of these PKC isozymes, which binds diacylglycerol (DG) or the functional analogues, phorbol esters (3). The intrinsic membrane affinity of the C1 domain of conventional PKC isozymes is 2 orders of magnitude lower than that of the novel PKC isozymes (4, 5), and effective membrane translocation is only achieved following pre-targeting of PKC to the membrane by engaging its Ca^{2+}-dependent C2 domain (6). For novel PKC isozymes, the affinity of their C1 domain is sufficiently high that agonist-evoked changes in diacylglycerol are sufficient to recruit novel PKCs to the membrane. Engaging the C1 domain (and C2 domain for conventional PKCs) provides the energy needed to release an autoinhibitory pseudosubstrate sequence from the active site, thereby allowing phosphorylation of substrates. Imaging of PKC activity and DG production in real time in live cells with FRET-based reporters has revealed that PKC activity is localized to those cellular locations where DG is generated (7, 8). Thus, PKC has served as a paradigm for an enzyme that is reversibly activated by membrane binding.

The C1 domain is a small (~8 kDa) globular domain, rich in β-sheet and requiring two Zn^{+2} ions for proper folding and stability. The DG/phorbol ester-binding site is formed by an "unzipped" β-sheet that is lined with hydrophobic residues. Crystallographic data revealed that binding to phorbol 12-myristate 13-acetate (PMA) is mediated through the backbone amides and carbonyls of Thr^{12}, Leu^{21}, and Gly^{23} (consensus residue numbering), rather than specific contacts with amino acid side chains; however, hydrophobic contacts between phorbol and the C1 domain reinforce the high affinity binding. This study also revealed that rather than alter the structure of the C1 domain, phorbol provides a greasy cap to facilitate binding of the domain to membranes. Moreover, despite being largely hydrophobic, the C1 domain has a ring of basic residues around its center, which may facilitate its interaction with anionic membranes (9, 10).

* This work was supported by National Institutes of Health Grants GM-43154, 2T32 GM-07752, and 2T32 GM-08326. The costs of publication of this article were defrayed in part by the payment of page charges. This article must therefore be hereby marked "*advertisement*" in accordance with 18 U.S.C. Section 1734 solely to indicate this fact.

[S] The on-line version of this article (available at http://www.jbc.org) contains supplemental Figs. S1–S4 and Tables SI–SIII.

[1] Current address: Center for Basic Neuroscience, University of Texas Southwestern Medical Center, 6000 Harry Hines Blvd., Dallas, TX 75390-9111.

[2] To whom correspondence should be addressed: UCSD, 9500 Gilman Dr., 0721, La Jolla, CA 92093-0721. Tel.: 858-534-4527; Fax: 858-822-5888; E-mail: anewton@ucsd.edu.

[3] The abbreviations used are: PKC, protein kinase C; DG, *sn*-1,2-dioleoylglycerol; PMA, phorbol 12-myristate 13-acetate; PG, phosphatidylglycerol; PS, phosphatidylserine; SLV, sucrose-loaded vesicle; PC, phosphatidylcholine; dansyl, 5-dimethylaminonaphthalene-1-sulfonyl.

The anionic phospholipid phosphatidylserine (PS) is a specific activator of PKC, with Hill coefficients as high as 12 noted for the activation of full-length enzyme in a mixed-micelle assay or 4 with lipid bilayers (11–15). Binding studies have revealed that the enzyme specifically binds and is activated by *sn*-1,2-phosphatidyl-L-serine and not the enantiomeric *sn*-2,3-phosphatidyl-D-serine, suggesting the existence of specific determinants on the enzyme that bind PS (16). This stereospecificity is retained in the isolated C1 domain, suggesting that PS binds specifically to this domain (17). The C2 domain also displays selectivity for PS over other anionic phospholipids (18, 19), but, in contrast to the C1 domain, this selectivity is not stereospecific (17).

Phorbol esters have long been known to be potent activators of PKC (20). PMA binds to the C1 domain in a similar qualitative manner to DG (21), however, PKC binds to PMA-containing membranes with 2 orders of magnitude higher affinity than to DG-containing membranes (5). The lower affinity binding to DG allows agonist-stimulated PKC signaling to be rapidly reversed (22), whereas phorbol ester treatment results in chronic activation (23), which, dependent on the PKC isoform activated, may lead to either cancer or growth inhibition and apoptosis (24). Equilibrium or monolayer penetration experiments have provided much information on how binding of C1 ligands recruits PKC to membranes (18, 25, 26). Moreover, early studies described a qualitative difference in the binding affinities and activation potencies between DG and a variety of phorbol esters (27). To date, however, a kinetic mechanism describing what drives the association of the domain to membranes and retention on membranes has not been addressed.

We have recently shown that a single amino acid in the C1 domain (at position 22) tunes the affinity of this domain for DG-containing membranes (4). This residue lies on the outside face of one of the sides of the ligand binding pocket. When present as Trp, as it is in novel PKC isozymes, the domain binds DG-containing membranes with sufficiently high affinity to sense agonist-evoked generation of DG. When present as Tyr, as it is in conventional isozymes, the affinity for DG-containing membranes is an order of magnitude lower, thus requiring a second targeting mechanism (Ca^{2+}-dependent engagement of the C2 domain) for translocation to membranes. In this study, we take advantage of engineering a Trp at the tuning position of a conventional PKC to obtain a C1 domain that now has a high membrane affinity and a built-in fluorophore.

We report on the kinetics for the interaction of the isolated C1 domain with lipid membranes, examining the role of PS and C1 ligand in the association and dissociation rate constants. The kinetic data provide evidence for a two-step mechanism by which the C1 domain interacts with membranes: an initial recruitment through electrostatic interactions with PS followed by a secondary search for ligand in two dimensions. High affinity interactions with membranes are determined by the extent to which hydrophobic interactions are productively made in this second step. This model explains in part the transient nature of DG signaling *versus* the chronic nature of PMA signaling and provides a framework for the rational design of PKC modulators.

EXPERIMENTAL PROCEDURES

Materials—1-Palmitoyl-2-oleoyl-*sn*-glycero-3-phosphocholine (PC), 1-palmitoyl-2-oleoyl-*sn*-glycero-3-phospho-L-glycerol (PG), PS, and DG in chloroform were from Avanti Polar Lipids, Inc. L-α-Dipalmitoyl,[2-palmitoyl-9,10-^{3}H]phosphatidylcholine (60 Ci mmol^{-1}) was from American Radiochemical Co. PMA was from CalBiochem. Chelex 100 was purchased from Sigma. Electrophoresis reagents were from Bio-Rad Laboratories, Inc. All other reagents and chemicals were reagent grade.

Cloning and Purification of C1bβ-Y123W—Rat C1bβ-Y123W was subcloned into pGEX-6P3 and bacterially expressed and purified as described previously (4). Untagged domain was used for all experiments.

Preparation of Lipid Vesicles—Sucrose-loaded vesicles (SLVs) were prepared as described (5); lipid vesicles for stopped-flow spectroscopy were prepared as described (6). PMA was included as a lipid component in the calculation of the mole % of each desired lipid. PC was used as a neutral diluent to comprise the remaining mole % of phospholipid. The final concentration of lipid was determined by phosphate analysis as described (28). Lipid concentrations of DG-containing vesicles were calculated by dividing the phospholipid concentration by a factor of (1 minus the mole fraction of DG). PMA was incorporated into these vesicles as described (5).

Steady-State Fluorometry—Steady-state tryptophan fluorescence data were collected using a Jobin (Edison, NJ) Yvon-SPEX FluoroMax-2 fluorescent spectrometer using constant wavelength analysis. Data were collected at 25 °C by excitation at 280 nm and monitoring emission at 340 nm. Solutions were successively added to an EDTA-treated 10-mm rectangular quartz cuvette with stirring (Starna Cells, Inc.) and were allowed to equilibrate for at least 2 min before recording fluorescence. Experiments were conducted in triplicate, correcting the mean emission intensity for the added sample volume.

SLV Binding Assay—The binding of the C1b domain to SLVs and subsequent analysis was as described previously (4). When used, K_d^{SLV} designates equilibrium constants derived from these assays.

Stopped-flow Fluorescence Spectroscopy—Kinetic traces were measured using an Applied Photophysics Π^*-180 stopped-flow fluorescence spectrometer (Leatherhead, UK). Kinetic analysis for the biomolecular association between the C1b domain and lipid vesicles (Equation 1) was conducted as described previously (6).

$$\text{C1b}\beta + \text{lipid} \leftrightarrow \text{C1b}\beta \cdot \text{lipid} \qquad \text{(Eq. 1)}$$

Lipid concentrations were chosen to be similar to those used in the equivalent SLV assay. For association experiments, final protein concentrations were 10-fold below the lowest lipid concentration tested. All experiments were temperature-controlled through the use of a 25 °C circulating water bath. All solutions were prepared in Chelex-treated buffer containing 20 mM HEPES, pH 7.5, 150 mM NaCl, 200 μM $CaCl_2$, and 1 mM dithiothreitol prior to mixing. Treatment of buffer with Chelex was critical for the acquisition of monoexponential fits for all traces; untreated buffer often gave irreproducible fits deviating

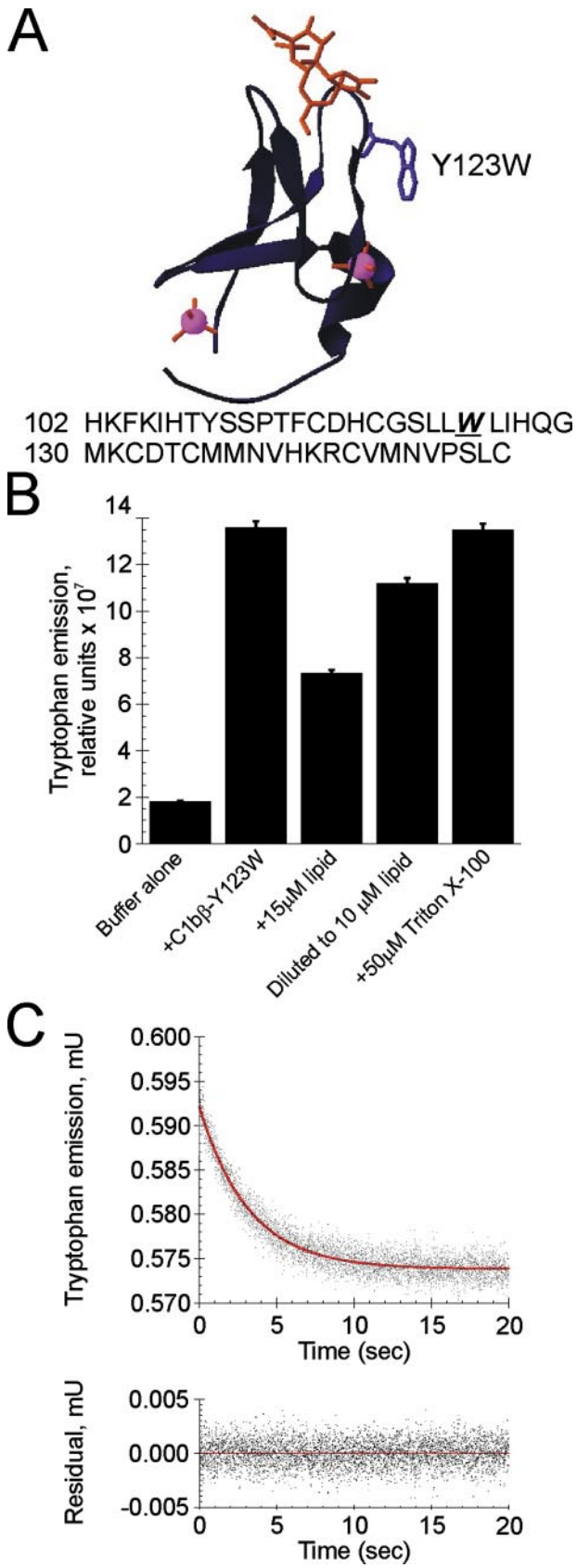

FIGURE 1. **C1bβ-Y123W can be used as a fluorescent probe for binding to lipid vesicles.** *A*, homology model and sequence of C1bβII-Y123W. The primary sequence of the C1b domain of human PKCβII was modeled by homology onto the crystal structure of the C1b domain of mouse PKCδ (Protein Data Bank code 1PTR) using Swiss PDB-Viewer. The ribbon structure of C1bβII-Y123W is in *navy blue*; the structural zinc ions in *lavender*; phorbol in *orange*; and the Y123W mutation indicated in *light blue*. The primary amino acid sequence is shown below, with the engineered Trp^{123} highlighted. *B*, 0.2 μM C1bβ-Y123W was added to Chelex-treated buffer containing 150 mM NaCl, 200 μM $CaCl_2$, 1 mM dithiothreitol, and 20 mM HEPES, pH 7.4, and tryptophan fluorescence was monitored by emission at 320 nm. The diluent used to dilute the lipid to 10 μM contained 0.2 μM C1bβ-Y123W in the same buffer described above to keep constant the concentration of all other components. Addition of lipid and Triton X-100 solutions were in volumes less than 1% of the total volume, thus minimizing any effects on concentrations of the remaining components. The indicated solutions were added successively, and fluorescence was read after an incubation time of at least 2 min between additions to allow equilibrium to be reached. Vesicles were composed of 5 mol % PMA and 30 mol % PS. *C*, sample kinetic curve for the association of C1bβ-Y123W with lipid vesicles containing 5 mol % PMA and 40 mol % PS. Fluorescence >320 nm was monitored through a 320-nm high pass filter. The data are fit to a monoexponential decay curve describing the quenching of tryptophan fluorescence in this binding reaction. Residuals are plotted *below* the kinetic trace.

significantly from monoexponential decay. All curve fitting was done using KaleidaGraph version 5.32. When used, K_d^{calc} designates equilibrium constants calculated as the ratio of $k_{off}^{app}/k_{on}^{app}$.

RESULTS

Design of a Fluorescence-based Probe for the Interaction of the C1b Domain of PKCβ with Lipid Membranes—To study the kinetics of the association of the C1 domain with lipid vesicles using stopped-flow fluorescence spectroscopy, it was first necessary to design a fluorescence-based probe that was sensitive to such an interaction. We chose the C1b domain of the conventional isoform PKCβI/II because the isolated domain is stable and amenable to biochemical studies (5, 16, 17, 29); it is also part of a conventional PKC isoform whose biochemical and biophysical properties have been well studied (3, 5, 12, 13, 17, 29–31). (This domain will hereafter be referred to as C1bβ, as the C1b domain is identical in both isoforms.) This C1b domain does not contain an endogenous Trp fluorophore, thus we introduced Trp at four positions in the domain: F114W, H117W, Y123W, and L150W (PKCβII numbering). Only one construct, C1bβ-Y123W, underwent measurable changes in fluorescence upon membrane binding (Fig. 1*A*). Specifically, intrinsic Trp fluorescence was quenched upon binding to model membranes. (This quenching upon membrane binding prevented fluorescence resonance energy transfer to dansyl-labeled lipids, an output that has been useful to study the membrane kinetics of the C2 domain (6); thus we focused on Trp quenching to monitor membrane binding.) Subsequently, we discovered that this mutation tunes the affinity of the domain for diacylglycerol, but not phorbol esters (4). Thus, the construct used in this study has the advantage of binding DG with sufficiently high affinity to be capable of sensing agonist-evoked diacylglycerol.

Fig. 1*B* shows that the intrinsic tryptophan fluorescence of C1bβ-Y123W decreased by ~50% upon addition of vesicles predicted to result in ~80% bound domain (15 μM total lipid; 30 mol % PS, 5 mol % PMA, 65 mol % PC) (17). Trp emission was fully restored upon complete dissociation of C1bβ-Y123W from lipid vesicles by the addition of detergent. Moreover, quenching of Trp fluorescence was reversible; fluorescence was recovered upon dilution of lipid to a concentration predicted to result in ~50% bound domain (10 μM). Finally, despite being

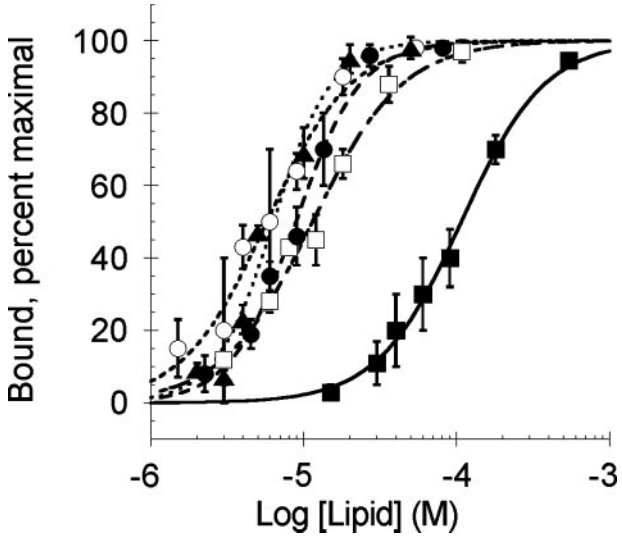

FIGURE 2. **PS increases the affinity of C1bβ-Y123W for PMA-containing lipid vesicles 10-fold.** Binding of C1bβ-Y123W to lipid vesicles containing 5 mol % PMA and increasing mole % PS as follows (remainder PC): 0 (■), 10 (□), 20 (●), 30 (○), and 40 (▲). Each data point represents the mean of triplicate experiments ± S.E.

highly soluble and able to bind vesicles, none of the three other Trp mutants displayed this property indicating that the decrease in Trp emission is a specific property of C1bβ-Y123W and not a nonspecific effect of the experimental conditions, *e.g.* light scattering by lipid (data not shown).

We next examined the association of C1bβ-Y123W with lipid vesicles using stopped-flow fluorescence spectroscopy. Trp quenching was monitored following the mixing of C1bβ-Y123W with vesicles containing 5 mol % PMA and 40 mol % PS (remainder PC). Traces for the association of the domain with lipid were monoexponential (Fig. 1*C*, *top*), with residuals consistent with simple, monophasic kinetics (Fig. 1*C*, *bottom*). Control experiments in which protein or lipid alone was rapidly mixed with buffer showed no change in fluorescence up to 40 s (data not shown). As another control, identical experiments with mutants C1bβ-F114W, -H117W, and -L150W did not show any time-dependent change in Trp emission (data not shown). These data demonstrate that the Trp fluorescence of the C1bβ-Y123W construct serves as a direct readout for the binding of the C1 domain to lipid vesicles.

Binding of C1bβ-Y123W to Vesicles Containing Increasing Mole % PS—The interaction of PKC with PS is stereospecific and displays high cooperativity. Previous studies revealed that the determinants for the stereospecific interaction of PKC with PS reside within the C1 domain (3, 16, 17). Thus, we set out to address the kinetic basis for this specificity. First, we examined the equilibrium binding of the C1bβ-Y123W construct to sucrose-loaded vesicles. The binding curves in Fig. 2 illustrate the exquisite sensitivity of binding to PS content: the presence of 10 mol % PS increased the affinity of C1β-Y123W for lipid vesicles 10-fold compared with the affinity for vesicles without PS (K_d^{app} = 9.8 ± 0.3 for 10% PS *versus* 107 ± 8 μM for 0% PS). Further increasing the PS content to 40 mol % only increased the affinity for membranes 1.8-fold (K_d^{app} = 9.8 ± 0.3 μM for 10% PS and 5.3 ± 0.5 for 30% PS). Hill coefficients were similar

TABLE 1

Apparent equilibrium and kinetic parameters for the association of C1bβ-Y123W with lipid vesicles of increasing mole % PS

Vesicles were composed of 5 mol % PMA and the indicated mole % PS (remainder PC). Apparent K_d^{SLVc} and Hill coefficients were taken from the weighted, least-squares fit of the data in Fig. 2. Apparent k_{on} and k_{off} were taken as the slope and *y* intercepts, respectively, of the weighted, least-squares fit of plots of k_{obs} *versus* vesicle concentration in association experiments. k_{on} values are in terms of (M vesicles)$^{-1}$s^{-1}. K_d^{calc} was calculated as the ratio of apparent k_{off}/k_{on} and converted to μM lipid, assuming 90,000 lipids per vesicle. Values are presented as the average of at least three experiments ± S.E.

Mol % PS	Apparent K_d^{SLVc}	Hill coefficient	Apparent $k_{on} \times 10^9$	Apparent k_{off}	K_d^{calc}
	μM lipid		$M^{-1}s^{-1}$	s^{-1}	*μM lipid*
0	107 ± 8	1.7 ± 0.1	0.05 ± 0.02	0.13 ± 0.02	200 ± 100
10	9.8 ± 0.3	1.62 ± 0.08	0.22 ± 0.03	0.11 ± 0.01	45 ± 7
20	8.4 ± 0.5	2.1 ± 0.2	0.22 ± 0.03	0.04 ± 0.02	16 ± 8
30	5.3 ± 0.5	1.6 ± 0.2	1.05 ± 0.06	0.090 ± 0.003	7.7 ± 0.5
40	6.3 ± 0.5	2.3 ± 0.4	1.62 ± 0.09	0.063 ± 0.004	3.5 ± 0.3

for all PS concentrations and ranged from 1.6 ± 0.2 to 2.3 ± 0.4, revealing some cooperativity in the membrane interaction.

Next, we examined the kinetics of interaction of the C1bβ-Y123W construct with membranes containing increasing mole % PS by stopped-flow fluorescence spectroscopy (Table 1, *right*). Association rate constants (k_{on}^{app}) increased dramatically with increasing mole % PS: we observed a 30-fold increase in association rate constant from 0.05 ± 0.02 × 10^9 M^{-1} s^{-1} for 0% PS to 1.62 ± 0.09 × 10^9 M^{-1} s^{-1} for 40 mol % PS. Moreover, the presence of PS in PMA-containing membranes pushed the rate of association to diffusion-limited values. Dissociation rates (k_{off}^{app}) decreased only slightly with increasing mole % PS and varied 3-fold at most, with the lowest being 0.04 s^{-1} for 20% PS and the highest being 0.13 ± 0.02 s^{-1} for 0% PS (Table 1). The dissociation rate constants in Table 1 were obtained from the *y* intercepts of the linear plots of k_{obs} *versus* lipid concentration in association experiments; direct measurements of k_{off} by dilution and competition experiments confirmed the values from association experiments (supplemental Fig. S1 and supplemental Tables SI and SII). Thus, the association of C1bβ-Y123W with PS-containing vesicles is exquisitely sensitive to PS, whereas the residence time on the membrane is only weakly sensitive to PS content.

Sensitivity to Ionic Strength of the Interaction of C1bβ-Y123W with Lipid Vesicles—Because the association of C1bβ-Y123W with lipid vesicles showed a strong dependence on mole % PS, the sensitivity of this interaction to ionic strength was tested. The interaction of C1bβ-Y123W with vesicles containing 5 mol % PMA and 20 mol % PS was relatively insensitive to KCl concentrations between 150 and 300 mM (Fig. 3, *left*). One possible interpretation of these data is that the membrane affinity is so high it masks any ionic strength sensitivity; therefore, the same interaction was tested under low affinity conditions (0.1 mol % PMA). Despite the 20-fold lower affinity of C1bβ-Y123W for 0.1 mol % PMA/20 mol % PS vesicles (supplemental Table SIII), this interaction, too, remained insensitive to ionic strength (Fig. 3, *right*). Moreover, initial kinetic experiments showed no effect of ionic strength on the association (k_{on}^{app}) or dissociation (k_{off}^{app}) rates of C1bβ-Y123W with lipid vesicles (data not shown). It is possible that sensitivity of this interaction to ionic strength would only be observed at much lower salt concentrations, as previously reported for ligand binding to acetylcholinesterase

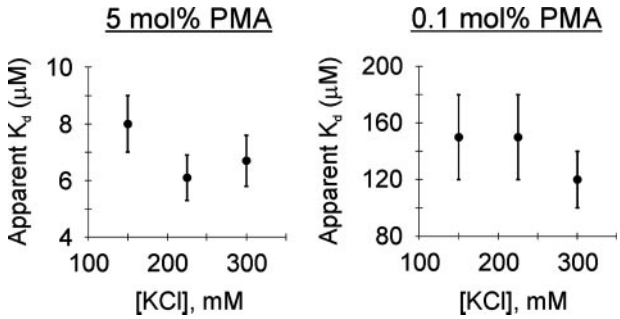

FIGURE 3. **The association of C1bβ-Y123W with lipid vesicles containing 0.1 (*left*) or 5 (*right*) mol % PMA and 20 mol % PS is not sensitive to ionic strength above 150 mM KCl.** The percent C1bβ-Y123W bound was determined by the SLV assay at a fixed lipid concentration corresponding to ~50% bound, *i.e.* 150 and 10 μM for 0.1 and 5 mol % PMA, respectively. Apparent K_d values were determined by using the Hill coefficient (n) for 150 mM KCl for each case (*i.e.* 1.3 and 2.1, respectively; see supplemental Table SIII) according to the equation: fraction bound = $[L]^n/([L]^n + K_d^n)$. Each data point represents the mean of triplicate experiments ± S.E.

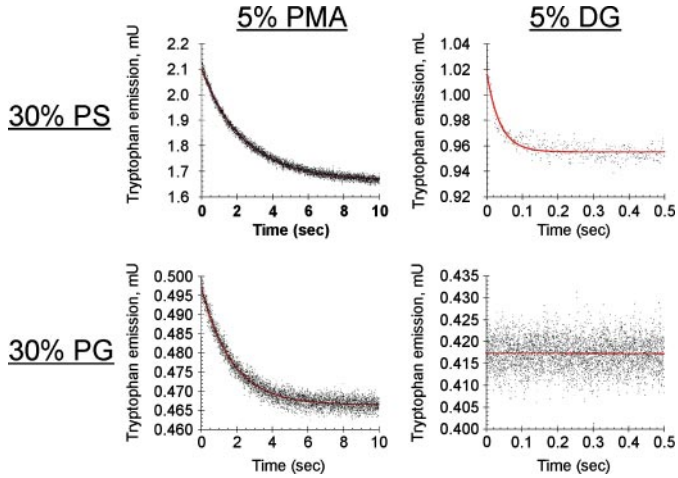

FIGURE 4. **Sample traces for the association of C1bβ-Y123W with lipid vesicles containing 5 mol % PMA (*left panels*) or 5 mol % DG (*right panels*) and 30 mol % PS (*top panels*) or PG (*bottom panels*).** Traces represent lipid concentrations at ~10 times the apparent K_d for each condition. Each trace is fitted to a monoexponential decay in tryptophan emission.

TABLE 2

Apparent equilibrium and kinetic parameters for the association of C1bβ-Y123W with lipid vesicles of 5 mol % PMA and 30 mol % PS or PG

Vesicles were composed of 5 mol % PMA and 30 mol % of the indicated anionic phospholipid, with the remainder composed of PC. Tabulated results are as in Table I. Equilibrium data were taken from Ref. 4 and supplemental Fig. S2. Values are presented as the average of at least three experiments ± S.E.

Anionic phospholipid	Apparent K_d^{SLVc}	Hill coefficient	Apparent $k_{on} \times 10^9$	Apparent k_{off}	K_d^{calc}
	μM *lipid*		$M^{-1}s^{-1}$	s^{-1}	μM *lipid*
PS	5.3 ± 0.5	1.6 ± 0.2	1.05 ± 0.06	0.090 ± 0.003	7.7 ± 0.5
PG	6.0 ± 0.9	1.5 ± 0.3	0.67 ± 0.07	0.111 ± 0.005	15 ± 2

(32); however, aggregation of the domain at 50 mM NaCl precluded equilibrium and kinetic analyses below 150 mM NaCl.

Interaction of C1bβ-Y123W with PS and PG and the Nature of Chemical Quenching—The interaction of the C1 domain with anionic phospholipid is selective for PS over PG (3, 17). The mechanism of the interaction of the C1 domain with PS, however, has not been established. Therefore, we characterized this specific interaction through the use of equilibrium measurements and stopped-flow fluorescence spectroscopy. Earlier characterization of C1bβ-Y123W by equilibrium experiments revealed that this domain shows selectivity for PS over PG in the context of DG-containing vesicles; however, when the ligand is PMA, C1bβ-Y123W binds both PS- and PG-containing membranes equally well, even under moderate affinity conditions (4) (supplemental Figs. S2 and S3 and Table SIII). We began by analyzing the kinetics of the interaction of C1bβ-Y123W with PMA membranes containing 30 mol % of either PS or PG (Table 2). The association of C1bβ-Y123W with both PS- and PG-containing PMA membranes displayed monoexponential kinetics (Fig. 4, *left panels*). C1bβ-Y123W showed nearly a 2-fold reduction in the rate of association with PG vesicles compared with PS vesicles ($k_{on}^{app} = 0.67 \pm 0.07 \times 10^9$ *versus* $1.05 \pm 0.06 \times 10^9$ M^{-1} s^{-1}, respectively), yet the same domain dissociated from these vesicles at nearly the same rate ($k_{off}^{app} = 0.111 \pm 0.005$ and 0.090 ± 0.003 s^{-1}, respectively, Table 2). These data reveal that the selectivity for PS occurs in the association step of the domain with membranes.

Next, we sought to analyze the mechanism by which C1bβ-Y123W is selective for PS over PG in the presence of DG by measuring the kinetics of the association of this domain with lipid vesicles. However, C1bβ-Y123W gave no change in fluorescence over time when vesicles containing 5 mol % DG and 30 mol % PG were used (Fig. 4, *lower right panel*). One possible explanation for such an observation is that the affinity of C1bβ-Y123W for DG/PG-containing vesicles was not high enough for our detection. However, we could not detect any time-dependent change in fluorescence at lipid concentrations spanning 5 to 95% C1bβ-Y123W bound (as assayed by the SLV method) for vesicles containing both 30 and 40 mol % PG (supplemental Fig. S4 and data not shown). A second explanation for such an observation is that PS contributes to the quenching of Trp fluorescence in such a way that PG cannot. Therefore, we compared the kinetic data for the binding of C1bβ-Y123W to vesicles containing either 5 mol % PMA or DG and 30 mol % PS or PG under conditions in which ~90% C1bβ-Y123W was bound to vesicles (Fig. 4). Comparison of the signal-to-noise ratio of the resulting matrix showed that the efficiency of the chemical quenching of Trp fluorescence decreased in the order PMA/PS > PMA/PG ≫ DG/PS ⋙ DG/PG. Such data show that (i) PMA contributes maximally and (ii) PS contributes minimally to the quenching of Trp fluorescence, and (iii) PG cannot efficiently contribute to the quenching of Trp fluorescence. Unfortunately, however, these results also precluded the derivation of kinetic parameters describing the association of C1bβ-Y123W with PG vesicles in the context of DG-containing vesicles.

Interaction of C1bβ-Y123W with PMA Versus DG—The data from the previous section suggested that C1bβ-Y123W interacts differently with PMA- and DG-containing lipid vesicles. Indeed, previous studies had shown that PKC binds with 2 orders of magnitude higher affinity to PMA-containing vesicles than to DG-containing vesicles (4). Moreover, PMA and DG differ in both their binding to and activation of PKC (27). Therefore, we next used stopped-flow fluorescence spectroscopy to extract kinetic parameters for the interaction of C1bβ-Y123W with membranes containing 40 mol % PS and either 5 mol % PMA or DG (Table 3). 40 mol % PS was used for com-

TABLE 3

Apparent equilibrium and kinetic parameters for the association of C1bβ-Y123W with lipid vesicles of 40 mol % PS and either 5 mol % PMA or DG

Vesicles were composed of 40 mol % PS and 5 mol % of the indicated ligand, with the remainder composed of PC. Tabulated results are as in Table I. Equilibrium data were taken from the weighted, least-squares fit of the data in Fig. 5. Values are presented as the average of at least three experiments ± S.E.

5 mol % Ligand	Apparent K_d^{SLVc}	Hill coefficient	Apparent $k_{on} \times 10^9$	Apparent k_{off}	K_d^{calc}
	μM lipid		$M^{-1}s^{-1}$	s^{-1}	*μM lipid*
PMA	6.3 ± 0.5	2.3 ± 0.4	1.62 ± 0.09	0.063 ± 0.004	3.5 ± 0.3
DG	63 ± 3	1.4 ± 0.1	5.95 ± 0.03	14.20 ± 0.04	215 ± 1

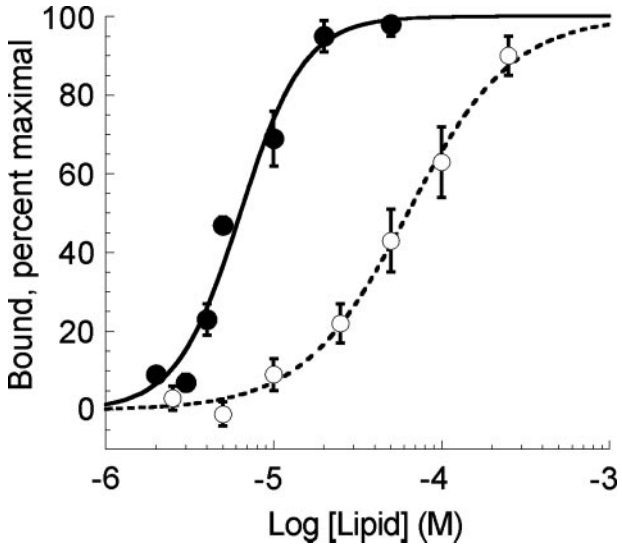

FIGURE 5. **C1bβ-Y123W binds PMA-containing vesicles with 10-fold higher affinity than DG-containing vesicles containing 40 mol % PS.** Binding of C1bβ-Y123W to lipid vesicles containing 40% PS and 5% PMA (●) or 5% DG (○). Each data point represents the mean of triplicate experiments ± S.E.

parisons, as this condition yielded more reliable data with a higher signal-to-noise ratio and better amplitudes (see previous section on the nature of chemical quenching). Again, the association and dissociation of C1bβ-Y123W with vesicles followed monoexponential kinetics. Equilibrium experiments revealed that C1bβ-Y123W bound to PMA-containing vesicles with 10-fold higher affinity than to DG-containing vesicles (Fig. 5). Despite this result, kinetic experiments revealed that C1bβ-Y123W associated with vesicles containing 5 mol % PMA nearly four times more slowly than with vesicles containing 5 mol % DG (k_{on}^{app} = 1.62 ± 0.09 × 10^9 *versus* 5.95 ± 0.03 × 10^9 M^{-1} s^{-1} for PMA and DG, respectively, Table 3). However, the slower association rate was outweighed by a dissociation rate over 200 times slower than from DG-containing vesicles to give a net increase in affinity for PMA-containing vesicles (k_{off}^{app} = 0.063 ± 0.004 *versus* 14.20 ± 0.04 s^{-1} for PMA and DG, respectively). Thus, for the unimolecular dissociation of C1bβ-Y123W from vesicles, the half-life for the retention of the domain at DG-containing membranes was only 0.05 s compared with 11 s when PMA was the ligand. Taken together, these data indicate that the residency time of the C1 domain on the membrane is primarily dependent on its interactions with its membrane-bound ligand.

DISCUSSION

This study identifies the determinants that control the association and dissociation of the C1 domain from membranes. Stopped-flow spectroscopy using the C1b domain of PKCβ, with an engineered Trp at position 123, reveals that membrane association is driven by electrostatic interactions with anionic lipids that are specifically enhanced when PS is present, and that membrane retention is driven by hydrophobic interactions that depend on the concentration and nature of C1 ligand. Thus, membrane association is highly sensitive to anionic lipid and relatively insensitive to C1 ligand, whereas membrane retention is relatively insensitive to anionic lipid and highly dependent on C1 ligand.

Kinetic studies reveal that in the absence of anionic lipid, the C1 domain associates with PMA membranes below its diffusion-limited value. The presence of 30 mol % anionic lipids enhances the association rate by 1 order of magnitude, with a further 2-fold enhancement upon specific interactions with PS. Furthermore, the presence of anionic lipids enhances the association rate so as to approach diffusion-limited association of the C1 domain with membranes. On the other hand, these same anionic lipids play only a minor role in retention of the C1 domain at the membrane, as 30 mol % anionic lipids reduce the dissociation rate by only 25%. Once at the membrane, however, the C1 domain does not discriminate between PS and PG, with both anionic lipids providing the same rate of dissociation. Surprisingly, comparison between membranes containing DG and its potent analogue PMA revealed a *decrease* in association rate with PMA membranes. The faster association rate with DG membranes may result from either the ease of binding a smaller ligand in DG or from specific recognition of a DG/PS complex or from both. Regardless of mechanism, the decrease in association rate with PMA membranes was offset by a 200-fold decrease in the dissociation rate, thereby giving a net 10-fold increase in affinity for PMA-containing membranes. Indeed, the latter is consistent with studies with full-length PKCβII that suggested a 200-fold reduction in k_{off} for PMA relative to DG (30). Overall, the results support a model in which the interaction between C1bβ-Y123W and lipid membranes is mediated by a balance between electrostatic interactions with anionic lipids and hydrophobic interactions with membrane-bound ligand (see below and Fig. 6).

The data here complement those from many elegant studies on the nature of the interaction of the C1 domain with lipid membranes (18, 25–27, 33, 34). Many of these studies, however, rely on tagged domains or full-length proteins and/or rely on a semi-rigid, two-dimensional plane of membrane, such as a microchip or lipid monolayer. The present study, however, provides direct kinetic parameters for the interaction of the isolated, untagged C1 domain with lipid vesicles. Moreover, these data agree with, quantify, and enhance previous membrane penetration data that described recruitment of the C1 domain to membranes by nonspecific electrostatic interactions followed by membrane penetration via hydrophobic interactions (34).

There is much controversial evidence over the location of PS specificity in PKC. *In vitro* studies on isolated domains have

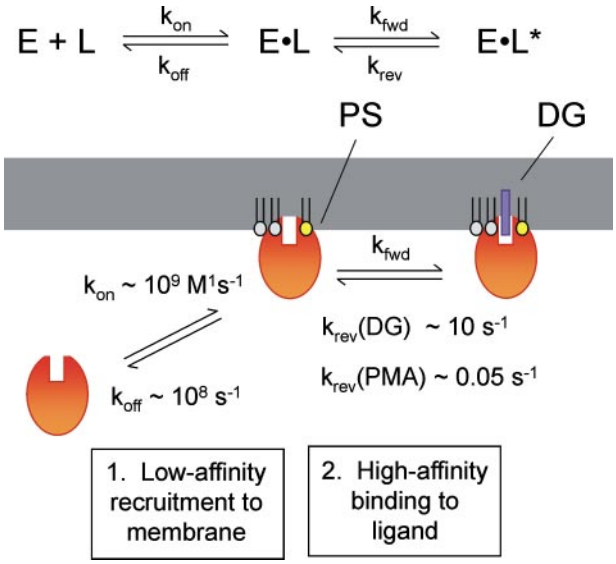

FIGURE 6. **Model for the interaction of the C1 domain with lipid membranes.** The proposed model for the interaction of the C1 domain with membranes occurs via two steps: the formation of a low affinity encounter complex followed by transition to a high affinity species (*above*). *Step 1*: long range, nonspecific electrostatic interactions with anionic lipids, such as PS (*yellow*), pre-target the C1 domain to the membrane through a diffusion-limited association and a rapid dissociation, resulting in a low affinity for membranes in the absence of DG or PMA. This weak recruitment to membranes facilitates the specific binding of the domain to DG or PMA by reducing the space in which the C1 must search for its ligand to two dimensions (26). *Step 2*: high affinity for ligand-containing membranes is achieved via coupling of this first weak equilibrium with a second, stronger interaction as the C1 domain searches along the lipid bilayer in two dimensions for specific interactions with its specific ligands: PS (*yellow*) and either PMA or DG (*purple*). The net rate of dissociation (dictated by k_{rev}) depends primarily upon hydrophobic contacts with the ligand, with 200-fold higher retention at PMA-containing membranes than DG membranes.

concluded that the C1 domain confers PS specificity, whereas nonspecific interactions exist between anionic phospholipid and the C2 domain (17). Equilibrium data presented here show that interaction of the C1 domain with membranes is selective for PS over PG only when the ligand is DG and not PMA. Two reasons may explain such an observation: 1) the C1 domain contains a binding pocket for the stereospecific recognition of DG/PS clusters or 2) the C1 domain has intrinsic selectivity for PS over PG regardless of ligand, but the affinity in the presence of PMA is very high, such that the 200-fold lower dissociation rate masks the effects of specific electrostatic interactions in the association with PS. Evidence for the former includes the faster association rate with DG membranes over PMA membranes and the observation that DG can cluster PS into microdomains in the lipid bilayer (35). Evidence for the latter, however, includes the observation here that PMA masks lower electrostatically driven association rates by driving down the dissociation rate 200-fold. Further evidence supporting the latter comes from our data showing (*a*) a slight preference for PS under low affinity conditions (supplemental Table SIII); (*b*) a 2-fold enhancement in the apparent rate of association with PS membranes (Table 2); and (*c*) the insensitivity to ionic strength under both low and high affinity conditions (Fig. 3). Indeed, when the PMA concentration is high relative to anionic lipid, ionic contributions to the interaction disappear, such that interactions with phorbol predominate (30). Unfortunately, the fluorescent reporter used in this study did not show time-dependent changes with DG/PG vesicles, thereby precluding the drawing of conclusions between PS and PG in the context of DG-containing vesicles. Taken together, the data support a model in which specificity in the association of the C1 domain with PS-containing *versus* PG-containing membranes is intrinsic to the domain regardless of ligand; however, the large contribution of PMA to the dissociation rate masks any such selectivity in the association rate, thereby resulting in a net apparent affinity that is similar for both PMA/PS- and PMA/PG-containing membranes.

The interaction of the C1 domain with membrane-bound ligand appears to be driven by hydrophobic interactions. DG and PMA share a glycerol-like backbone with two acyl chains, but PMA also contains an extensive, polycyclic, highly hydrophobic phorbol head group. X-ray crystallography revealed that rather than alter the overall structure of the domain, the main function of the ligand is to provide a greasy cap to promote the retention of C1 domain at the lipid bilayer (10). Indeed, the data here show a 200-fold slower rate of dissociation with the more hydrophobic PMA than the smaller DG. This difference corresponds to a difference of −3.2 kcal/mol in the dissociation rate, which, at a van der Waals interaction energy of 0.5 to 1.5 kcal/mol, could be explained as the energy of anywhere from two to six additional hydrophobic van der Waals interactions that do not exist in the interaction with DG. Indeed, the crystallographic data for C1bδ suggest that numerous hydrophobic interactions occur between C1bδ and the rings and acetyl group of the phorbol ester (10).

Whether the C1 domain penetrates substantially into the membrane is unresolved. Monolayer penetration experiments have suggested that hydrophobic residues within the C1 domain are responsible for pulling the C1 domain into the bilayer (18, 33, 34); however, quenching studies show no penetration of PKCβII into the acyl chains of the lipid bilayer (30). Our results reveal that PS can quench Trp fluorescence but PG cannot; similarly PMA can quench Trp fluorescence but DG cannot. Two possibilities could account for these observations: (i) different interactions between the two sets of ligands and (ii) intrinsic inability of the latter of the pairings to quench Trp fluorescence. Whereas we cannot rule out the former, the latter (ii) is an interesting possibility. Indeed, the unsaturated rings of phorbol would be ideal for scavenging the energy released by a neighboring fluorophore. In fact, phorbol ester appeared to be the largest contributor to the quenching phenomenon (Fig. 4). Moreover, because neither the glycerol backbone with acyl chains (*i.e.* DG) nor PG quenches Trp fluorescence, this suggests that either the amine or carboxylic acid functionalities of PS can also quench Trp emission. Indeed, Trp prefers to sit at the membrane/water interface rather than project into the membrane (36, 37). Thus, the data in this study are consistent with interactions between Trp and chemical quenchers at the level of lipid head group and are inconsistent with membrane penetration.

Model for the Interaction of the C1 Domain with Anionic Membranes—All association and dissociation experiments revealed monoexponential kinetics in the interaction of the C1 domain with membranes, thereby giving the appearance of a

simple binding equilibrium with a single bimolecular association and single unimolecular dissociation step, *i.e.* $E + L \leftrightarrow E{\cdot}L$. However, the dissociation constants from equilibrium (K_d^{SLV}) and kinetic ($K_d^{calc} = k_{off}^{app}/k_{on}^{app}$) experiments did not agree with one another in nearly all experiments (Tables 1–3). Cooperativity alone could not reconcile the differences between these two K_d values, suggesting a more complicated binding scheme than that outlined above. One explanation for this difference is that the kinetic scheme is more complicated than the single binding equilibrium presented above. Specifically, there may be an additional binding step that does not result in a fluorescence change in the reporter or, alternatively, the association or dissociation step could comprise two steps so similar in rate that they cannot be graphically resolved.

Based on the above data, we propose a model in which the C1 domain binds to DG- or PMA-containing membranes via a two-step mechanism consisting of the formation of a weak encounter complex (Step 1: $E + L \leftrightarrow E{\cdot}L$) coupled to a transition equilibrium in which high affinity, ligand-bound complex is formed (Step 2: $E{\cdot}L \leftrightarrow E{\cdot}L^*$, Fig. 6). Such a scheme is consistent with data showing that the binding of two proteins involve the formation of a weak, pre-equilibrium complex, followed by relaxation into a high affinity, stereospecific complex (38). The above model describes the binding equilibrium in terms of four rate constants: two that describe the initial low affinity recruitment to membranes (k_{on} and k_{off}) and two that describe the equilibrium for the formation of a high affinity transition complex (k_{fwd} and k_{rev}). Under such a scheme, the kinetically derived association and dissociation rate constants from stopped-flow experiments are apparent (k_{on}^{app} and k_{off}^{app}) and contain components of both Steps 1 and 2.

The affinity of the C1 domain for lipid membranes in the absence of ligand (*i.e.* DG or PMA) is ~100 mM (3); this K_d is equal to k_{off}/k_{on} and thus describes the recruitment equilibrium of Step 1. Assuming that the initial encounter of the C1 domain with acidic membranes is diffusion limited ($k_{on} \approx 10^9\ M^{-1}\ s^{-1}$), then $k_{off} \approx 10^8\ s^{-1}$, consistent with a weak affinity when the hydrophobic tethering forces of DG or PMA are absent. Moreover, if we assume that Step 1 is in rapid equilibrium, then $k_{off}^{app} = k_{rev}$, and k_{on}^{app} is the net rate constant for formation of $E{\cdot}L^*$. Extrapolation of the data presented here, then, allows us to estimate k_{fwd} at $\approx 10^2$–$10^3\ s^{-1}$ for both DG and PMA-containing membranes (data not shown).

The model in Fig. 6 highlights several important contributions to the interaction of the C1 domain with membranes. First is the importance of anionic lipids in the initial recruitment step. This is demonstrated by two observations: (*a*) in the absence of PS, the C1 domain associates with membrane vesicles below its diffusion-controlled value (Table 1); and (*b*) vesicle-binding experiments reveal that the C1 domain from PKCζ, which has a higher electrostatic potential than C1bβ (39), does not have a higher intrinsic affinity for PS membranes in the absence of DG or PMA,[4] thus suggesting that the C1 domain is already optimized for electrostatic interactions with membranes. A second contribution to the interaction of the C1 domain with membranes is the rapid ($\sim 10^2$–$10^3\ s^{-1}$) search for ligand that can occur upon a reduction in dimensionality that results from the initial encounter with membranes. In fact, this is a shared feature for the high affinity binding of many membrane-binding domains (26). A third contribution to binding is the "tethering" effect that hydrophobic interactions provide for the high affinity of the interaction of the C1 domain with membranes. This is demonstrated by the observation that k_{rev} is rate-limiting in the release of the C1 domain from DG- and PMA-containing membranes and varies from 10 s^{-1} for DG to 0.05 s^{-1} for PMA.

Taken together, then, the measured k_{on}^{app} values are consistent with a rate-limiting, diffusion-controlled association driven by electrostatic interactions between the positive electrostatic potential of the C1 domain and the negatively charged phospholipid bilayer. Moreover, the rate of release is limited by the extent to which the C1 domain makes hydrophobic contacts with ligand.

Conclusion—Dissection of the association and dissociation rates for binding of the C1 domain with membranes have revealed a two-step model for the translocation of the C1 domain to membranes: (i) anionic phospholipids, specifically PS, drive the formation of an initial low affinity complex between the domain and membranes, followed by (ii) a transition to a high affinity interaction when the C1 ligand is bound to the domain. The data reveal that the interaction of C1bβ-Y123W with DG-containing membranes is optimized for rapid, transient interactions, whereas PMA chronically locks the C1 domain to the membrane.

Acknowledgments—We thank Dr. Susan Taylor for use of the Fluoro-Max-2 fluorescent spectrometer, Dr. Patricia Jennings for use of the Π**-180 stopped-flow fluorescence spectrometer, Dr. Eric Nalefski for preparation of several C1bβ mutant constructs, and Dr. Joseph Adams for helpful discussions in the preparation of this manuscript.*

[4] D. R. Dries and A. C. Newton, unpublished observations.

REFERENCES

1. Newton, A. C. (1995) *J. Biol. Chem.* **270,** 28495–28498
2. Nishizuka, Y. (1986) *Science* **233,** 305–312
3. Newton, A. C. (2001) *Chem. Rev.* **101,** 2353–2364
4. Dries, D. R., Gallegos, L. L., and Newton, A. C. (2007) *J. Biol. Chem.* **282,** 826–830
5. Giorgione, J. R., Lin, J. H., McCammon, J. A., and Newton, A. C. (2006) *J. Biol. Chem.* **281,** 1660–1669
6. Nalefski, E. A., and Newton, A. C. (2001) *Biochemistry* **40,** 13216–13229
7. Gallegos, L. L., Kunkel, M. T., and Newton, A. C. (2006) *J. Biol. Chem.* **281,** 30947–30956
8. Violin, J. D., Zhang, J., Tsien, R. Y., and Newton, A. C. (2003) *J. Cell Biol.* **161,** 899–909
9. Hurley, J. H., and Misra, S. (2000) *Annu. Rev. Biophys. Biomol. Struct.* **29,** 49–79
10. Zhang, G., Kazanietz, M. G., Blumberg, P. M., and Hurley, J. H. (1995) *Cell* **81,** 917–924
11. Newton, A. C., and Koshland, D. E., Jr. (1989) *J. Biol. Chem.* **264,** 14909–14915
12. Orr, J. W., and Newton, A. C. (1992) *Biochemistry* **31,** 4661–4667
13. Orr, J. W., and Newton, A. C. (1992) *Biochemistry* **31,** 4667–4673
14. Lee, M. H., and Bell, R. M. (1989) *J. Biol. Chem.* **264,** 14797–14805
15. Lee, M. H., and Bell, R. M. (1992) *Biochemistry* **31,** 5176–5182
16. Johnson, J. E., Zimmerman, M. L., Daleke, D. L., and Newton, A. C. (1998) *Biochemistry* **37,** 12020–12025

17. Johnson, J. E., Giorgione, J., and Newton, A. C. (2000) *Biochemistry* **39,** 11360–11369
18. Bittova, L., Stahelin, R. V., and Cho, W. (2001) *J. Biol. Chem.* **276,** 4218–4226
19. Corbalan-Garcia, S., and Gomez-Fernandez, J. C. (2006) *Biochim. Biophys. Acta* **1761,** 633–654
20. Colon-Gonzalez, F., and Kazanietz, M. G. (2006) *Biochim. Biophys. Acta* **1761,** 827–837
21. Sharkey, N. A., Leach, K. L., and Blumberg, P. M. (1984) *Proc. Natl. Acad. Sci. U. S. A.* **81,** 607–610
22. Codazzi, F., Teruel, M. N., and Meyer, T. (2001) *Curr. Biol.* **11,** 1089–1097
23. Koivunen, J., Aaltonen, V., and Peltonen, J. (2006) *Cancer Lett.* **235,** 1–10
24. Griner, E. M., and Kazanietz, M. G. (2007) *Nat. Rev. Cancer* **7,** 281–294
25. Stahelin, R. V., Digman, M. A., Medkova, M., Ananthanarayanan, B., Rafter, J. D., Melowic, H. R., and Cho, W. (2004) *J. Biol. Chem.* **279,** 29501–29512
26. Cho, W., and Stahelin, R. V. (2005) *Annu. Rev. Biophys. Biomol. Struct.* **34,** 119–151
27. Kazanietz, M. G., Krausz, K. W., and Blumberg, P. M. (1992) *J. Biol. Chem.* **267,** 20878–20886
28. Bartlett, G. R. (1959) *J. Biol. Chem.* **234,** 466–468
29. Giorgione, J., Hysell, M., Harvey, D. F., and Newton, A. C. (2003) *Biochemistry* **42,** 11194–11202
30. Mosior, M., and Newton, A. C. (1995) *J. Biol. Chem.* **270,** 25526–25533
31. Mosior, M., and Newton, A. C. (1998) *Biochemistry* **37,** 17271–17279
32. Radic, Z., Kirchhoff, P. D., Quinn, D. M., McCammon, J. A., and Taylor, P. (1997) *J. Biol. Chem.* **272,** 23265–23277
33. Ananthanarayanan, B., Stahelin, R. V., Digman, M. A., and Cho, W. (2003) *J. Biol. Chem.* **278,** 46886–46894
34. Medkova, M., and Cho, W. (1999) *J. Biol. Chem.* **274,** 19852–19861
35. Dibble, A. R., Hinderliter, A. K., Sando, J. J., and Biltonen, R. L. (1996) *Biophys. J.* **71,** 1877–1890
36. Khandwala, A. S., and Kasper, C. B. (1971) *Biochim. Biophys. Acta* **233,** 348–357
37. Killian, J. A., and von Heijne, G. (2000) *Trends Biochem. Sci.* **25,** 429–434
38. Tang, C., Iwahara, J., and Clore, G. M. (2006) *Nature* **444,** 383–386
39. Pu, Y., Peach, M. L., Garfield, S. H., Wincovitch, S., Marquez, V. E., and Blumberg, P. M. (2006) *J. Biol. Chem.* **281,** 33773–33788